OBSTACLE DENSITY ESTIMATION ACCORDING FROM THE RADAR CHANNEL MEASUREMENTS TO THE TECHNICAL VISION SYSTEM OF GROUND-BASED ROBOTIC COMPLEX

DOI: 10.36724/2072-8735-2026-20-2-55-64

Manuscript received 02 December 2025;
Accepted 10 February 2026

Danil N. Bezumnov,
Moscow Technical University of Communications and Informatics, Moscow, Russia, ***d.n.bezumnov@mtuci.ru***

Denis S. Chirov,
Moscow Technical University of Communications and Informatics, Moscow, Russia, ***d.s.chirov@mtuci.ru***

Keywords: *robotic complex, technical vision system, radar measurements, information processing, object recognition*

One of the main trends in the development of robotics is the increasing autonomy and intellectualization of robotic complexes. The main source of data for decision-making and implementation of certain actions by the ground-based robotic complex (GBRC) is the technical vision system (TVS). Therefore, improving the TVS and data processing algorithms is an important task. The article presents the results of research on estimating the density of an obstacle based on measurements of the radar channel of the TVS of the GBRC. This task is relevant when the GBRC builds its route autonomously, i.e., when the GBRC builds its route from point A to point B and adjusts it if obstacles are detected. It is obvious that if the GBRC is used in a rural area, the optical channel will perceive tall grass as an obstacle and start rearranging the route, which may result in a longer path or, ultimately, the GBRC not completing its task. An analysis of existing studies has shown that it is possible to estimate the density of an obstacle using measurements from a mm-range radar system (RS). The results of evaluating the possibility of determining the density of obstacles using the radar channel of the onboard TVS of the GBRC using a simulation model of the radar channel showed that the density of obstacles can be estimated based on the normalized radar cross-section (RCS) of various obstacles. The normalized RCS of obstacles is determined with the least errors at short distances (about 10-15 m). Certain types of obstacles (trees, shrubs, and tall grass) can be further selected based on the correlation time of the received signal, which is significantly lower than that of homogeneous solid obstacles (wooden or concrete walls, and cars). The principle of using normalized RCS and signal correlation time depends on the type of classifier (artificial neural network, decision tree, etc.). Further research by the authors will focus on the specific implementation of this algorithm.

Information about authors:

Danil N. Bezumnov, *Moscow Technical University of Communications and Informatics, senior lecturer, Moscow, Russia*

Denis S. Chirov, *Moscow Technical University of Communications and Informatics, head of department, doctor of technical sciences, professor, Moscow, Russia*

Для цитирования:

Безумнов Д.Н., Чирова Д.С. Оценка плотности препятствия по измерениям радиолокационного канала системы технического зрения наземного робототехнического комплекса // T-Comm: Телекоммуникации и транспорт. 2026. Том 20. №2. С. 55-64.

For citation:

D.N. Bezumnov, D.S. Chirov, "Obstacle density estimation according from the radar channel measurements to the technical vision system of ground-based robotic complex," *T-Comm*, 2026, vol. 20, no. 2, pp. 55-64.

Introduction

Modern technical vision systems (TVS) for ground-based robotic complex (GBRC) are complex systems with a variety of multi-range sensors [1, 2]. Optical, infrared, and radar sensors are the most commonly used sensors in TVS [3]. Each measurement channel has its own advantages and disadvantages [4]. For example, an optical channel, which usually consists of several video cameras, can provide high-detail images in real time. However, passive optical sensors can only work in conditions of sufficient illumination, i.e., during the day and in the absence of interfering weather phenomena (fog, rain, etc.). The infrared channel (thermal imager) allows us to receive images of our surroundings at night, but the image quality and range will be much lower than those of an optical imager. It is the specific features and limitations of various sensors that have led to the fact that the TVS of the GBRC is a complex of multi-range sensors that are combined into a single system through the integrated processing of multi-range data [5, 6].

A large number of papers have been devoted to the problem of selecting an optimal (rational) set of sensors [7-9]. These studies have shown that in addition to sensors for obtaining visual information (images), the TVS of the GBRC should include devices for measuring the parameters of the observed objects: range, speed, etc. One of the interesting properties of observed objects is their density. This property is especially relevant for GBRC when they are building a route autonomously, i.e., when the GBRC builds a route from point A to point B and adjusts it if obstacles are detected. Obviously, if the GBRC is used in a rural area, the optical channel will perceive tall grass as an obstacle, and the GBRC will start rearranging the route. Obtaining radar or infrared images will not solve the problem either. Recognizing grass from images won't provide the desired result either, as there's no guarantee that there isn't a large rock or a fallen tree in the grass that the TVS doesn't currently see.

The solution to this problem is to measure the density of the obstacle, which will allow the GBRC's onboard algorithm to make a rational decision about the route. The density of the obstacle can be measured using a special radar channel in the TVS of the GBRC.

1 Analysis research in the subject area

As mentioned above, the TVS's channels, including radar channels, are used not only to solve classical problems of determining the range and geometric parameters of environmental objects, but also to determine such characteristics as their density [10, 11], type of material [12-17], structure [18-21], electrical conductivity [22], and volume [13, 15]. At the same time, radar data can both complement optical channel data and be used independently.

Paper [10] proposes an approach to estimating forest cover density based on the combination of optical and radar satellite data. 411 parameters were extracted from sub-meter optical satellite images, synthetic aperture radar satellite images, and digital elevation model data, and 17 of them were selected to build an estimated model of vegetation density. Three different models have been developed: multiple stepwise regression; neural network; and decision tree-based. As a result, the accuracy of density estimation increases from 76.50% for optical images and 78.50% for radar images to 78.66% for both options. The neural network-based model achieved the highest overall accuracy (79.19%) and demonstrated excellent accuracy in estimating low tree cover density (75.37%), while the decision tree-based model using radar image features showed excellent accuracy in estimating medium density (87.46%). It is noteworthy that the integrated decision tree-based cubic model, which combines optical and radar data, achieved the highest accuracy in estimating high vegetation cover density (89.17%).

In [11], the possibility of detecting a human body dummy by changes in the acoustic field caused by various boundary conditions in the low and moderately low frequency ranges is investigated.

Paper [12] presents the results of modeling the transmission of infrasonic energy in the range from 3 to 5 Hz through various types of fabrics (cotton, linen, wool, and nylon) with different wave propagation properties. Depending on the refractive index, these materials have different acoustic transparency, which in turn affects the reflected acoustic power.

A large number of modern vision systems use millimeter-wave radars. These systems are used to solve a wide variety of tasks: determining the level of liquids in various tanks, calculating the volume occupied by solid materials, assessing the surface in industry, measuring and monitoring vibration [13].

A number of papers consider the use of millimeter wave radars for monitoring a variety of materials, as well as objects, without their direct destruction, i.e. without penetration. For example, [13] presents a scheme for identifying various materials, and this scheme also contains a radar operating in the millimeter wave range. Identification of materials is performed using a set of specific machine learning methods. Reflected radar signature is used for machine learning. To solve this problem, the scheme uses three approaches: convolutional neural networks (CNN), the k-nearest neighbor method, and the dynamic time distortion (DTW) method. The authors managed to achieve almost 100% accuracy for the classification of six types of materials. The paper also contains the results of a study on whether it is possible to calculate the volume of material classified a step earlier. The research is conducted for three different levels. The results showed a classification with 98% accuracy.

In [14], the use of synthetic aperture radar (SAR) is investigated, a technology often used to solve problems of this class. Based on the information from the SAR, the intensity of yield in each single pixel of the image is identified. At the first stage, synthetic radar data is calculated. For this purpose, the parameters that are characteristic of a broadband radar are used if it operates in searchlight mode and illuminates several scattering regions, and these regions differ in frequency characteristics. At the second stage, the data set is divided into frequency sub-ranges, and the variance is calculated for each pixel. Finally, at the final stage, an elementary classification analysis makes it possible to identify the yield intensity.

Wireless classification of various materials is demonstrated in [15]. For this purpose, a broadband CMOS receiver operating in the millimeter range is used in the work. The experiment is arranged as follows: power is transmitted through several solid materials at different distances from the receiver, then it is recorded by the receiver in the W-band, which corresponds to frequencies in the range of 75-110 GHz. Based on the obtained data, materials are classified into various categories using machine learning methods. Trained classifiers were used to predict the values of the type

of material and its thickness. As a result, the classification accuracy was 96% for the type of material and 88% for the thickness.

The material identification system is described in [16]. This system uses a portable 3D imaging radar system. In this system, a 3D brightness map of an object is sent to the CNN input, and at the output, the authors receive an assumption about the class of the object's material. The authors proved that this approach gives better results than using raw data coming from antennas.

In [17], the problem of classifying materials in a set of different plates using a Siamese network is solved. This network uses a similarity metric that is directly related to the distance to the object under study. This indicator takes small values for identical materials. If the objects are made of different materials, then the value of the similarity indicator also increases. The results were tested in the classification of four different materials, using a short-range radar operating at a frequency of 60 GHz. The classification accuracy was more than 99%.

In [18], the application of X-ray diffraction analysis to determine the characteristics of materials with a crystal lattice is considered. The following characteristics are investigated: structure, phase, texture, average grain size, crystallinity, deformation, crystal defects. The paper contains a comparative analysis of the latest scientific developments in such industries as pharmaceutical and glass industry, flaw detection, forensic examination, electronics and geology.

Paper [19] presents an imaging method that uses coherent scattered or diffracted X-rays to identify potentially harmful or prohibited building materials.

Paper [20] describes the basic physical interaction of electromagnetic waves in the range of wavelengths from decimeters to millimeters (in a vacuum, frequencies from 300 MHz to 300 GHz) with various objects hidden behind dielectric materials (paper, wood, ceramics, concrete, polymer materials, and fiber composites) for their detection and evaluation of various characteristics. Practical examples of determining the moisture content of porous materials and controlling the process of injection molding of polymers are provided. Special attention is paid to visualizing objects hidden under clothing that need to be detected with maximum speed and accuracy, such as weapons and explosives.

Paper [21] discusses the use of artificial neural networks and machine learning to interpret ground-based radar data, taking into account knowledge about the propagation of electromagnetic waves, material properties, and antenna theory. Paper [22] explores the use of passive RFID tags to determine the dielectric constant of a test material.

Thus, a review of methods for assessing the density of materials shows that the mm-range radar channel of the TVS of the GBRC can be used to solve this problem [23]. In order to assess this possibility and evaluate the numerical characteristics, the authors conducted mathematical modeling.

2. Mathematical model of the radar channel of the TVS of the GBRC

Almost all modern on-board radar systems of the TVS of the GBRC use complex broadband probing signals that provide high resolution in range and angular coordinate (Doppler frequency). Taking into account modern means of digital signal generation and processing, pulsed signals with intra-pulse linear frequency modulation (IFM) and signals with direct spectrum expansion are the most preferable for radar tasks. In our case, we will limit ourselves to signals with direct spectrum expansion.

Let's consider the mathematical description of the GBRC radar channel. It contains, firstly, a description of the surface to be located, secondly, the ways in which the probing signal interacts with the surface to be located, and thirdly, a description of the reflected signal. The interaction of the probing signal with the reflecting surface is the main component, because depending on this, both the reflecting surface itself and the initial data used to describe the signal after reflection are described.

Let's apply a certain approach that describes the GBRC radar channel from a mathematical point of view. There is a concept of an independent reflector in this approach. Then the reflecting surface is represented as a set of independent reflectors. When using this approach, the output signal of the system will be a superposition of elementary reflected signals [24]. When using this description, the channel is defined by the scattering function. This function represents the average power distribution of the reflected signal, described in a special coordinate system from the delay and from the Doppler frequency shift.

When modeling a useful signal in the multi–position radar system of the TVS of the GBRC, used to detect obstacles, the main thing is the stage of forming the input radio signals in each receiver from the probing radio signals of all transmitters. This will allow us to take into account important properties of the model. It should also take into account the propagation of signals on the highway, their scattering on obstacles of various types, primarily targets, as well as passive interference and reflection from the underlying surface [24, 28-31].

In such tasks, solutions in a general matrix form for a system consisting of M transmitters and N receivers have proven themselves well. In a specific case, these systems can work for both reception and transmission, so the coordinates of the individual transmitters and receivers will match.

Thus, a linear system with M inputs and N outputs is formed, whose signal transmission can be described by an $M \times N$ transfer function matrix $K(\tau,t)$. In this case, the output signal vector $S(t)$ is described by the time-domain convolution of the input (emitted) signal vector $X(t)$ and the transfer matrix $K(\tau,t)$:

$$S(t) = \int_0^{t_{\max}} K(\tau,t) X(t-\tau) d\tau,$$

where $t_{\max}$ – maximum duration of transmission characteristics.

Let's take the following for granted: the input signals of the system are samples from the output of the probing generator, which are taken with a certain modeling step $\Delta t = t_j - t_{j-i}$. At the same time, the receiver input responses are calculated in increments that do not contradict Kotelnikov's criterion for the simulation bandwidth. This term refers to a band that is unifying for all the bands that are occupied by the emitted signals.

Let's define the matrix of transfer characteristics in discrete form:

$$K = X_A \cdot K_{tr} \cdot G_m \cdot F_{PTm}(\alpha,\beta) \cdot L_{ak} \cdot \Delta f_{prm},$$

where n – index of receiving modules; m – index of transmitting modules; k – index of propagation paths taken into account during

modeling; $X_A = \frac{G_n F_{PTn}(\alpha,\beta)}{\Delta f_{prn}}$; G_m – gain of the transmitting antenna of the *m*-th transmitter; $F_{PTm}(\alpha,\beta)$ – normalized radiation pattern of the *m*-th transmitter's transmitting antenna; Δf_{prm} – bandwidth of the *m*-th transmitting module's probe signal; G_n – gain of the receiving antenna of the *n*-th receiver; L_{ak} – losses due to signal propagation in the atmosphere; $F_{PTn}(\alpha,\beta)$ – normalized radiation pattern of the *n*-th receiver's receiving antenna; Δf_{prn} – center frequency of the *n*-th receiving module bandwidth; K_{tr} – matrix of propagation coefficients of radio signals from the *m*-th transmitter to the *n*-th receiver input.

The following types of paths must necessarily be taken into account at the stage of constructing the distribution coefficient matrix:

1) Direct transmission of the transmitter's radio signal to the receiver's input, then

$$K_{tr} = \frac{1}{R} e^{-jk_{rn}R},$$

where *R* – the distance between two objects (in this case, between the transmitter and the receiver),

$$R = \sqrt{\left(X_{txm}(t_i) - X_{rxn}(t_i)\right)^2 + \left(Y_{txm}(t_i) - Y_{rxn}(t_i)\right)^2 + \left(Z_{txm}(t_i) - Z_{rxn}(t_i)\right)^2},$$

where X_{txm}, Y_{txm}, Z_{txm} – coordinates of the *m*-th transmitting module at the current time; X_{rxn}, Y_{rxn}, Z_{rxn} – coordinates of the *n*-th receiving module at the current time; *k* - propagation constant of the *m*-th transmitter.

2) ngle-time reflection of a radio signal from an object (target)

$$K_{tr} = \frac{1}{R_{txm-c}} e^{-jk_{rn}R_{txm-c}\sigma_c},$$

where *i* – the index for the targets; R_{txm-c} – distance between the transmitter and the *i*-th target; σ_c – target RCS value depending on the irradiation angle.

3) Radio sign scattering by the underlying surface.

Consider the signal emitted by the transmitting device and scattered by the underlying surface. Obviously, this signal has a strong influence on the response that is received at the receiver input. This signal is the sum of the signals that have been reflected from each elementary area of the surface. The surface sections here mean a rectangular facet, but it can also be a triangular facet and an edge. This circumstance significantly complicates calculations, as it increases the amount of calculations. The set of multiple point reflectors will be a model of the underlying surface. Let's assume that they (reflectors) are randomly distributed over the surface. Since the reflection is almost specular, the reflectors in the model are located at different heights.

A commonly used law for the distribution of reflectors in height is the normal distribution. The mathematical expectation in this case will be zero. The variance will correspond to the standard deviation of the surface heights σ_s:

$$w(h) = \frac{1}{\sqrt{2\pi}\sigma_c} e^{-\frac{h^2}{2\sigma_c^2}}.$$

The phase distribution of elementary reflectors is uniform over the *t* interval, and the RCS distribution occurs according to Rayleigh's law:

$$w(h) = \frac{\sigma_z}{\sigma_0^2} e^{-\frac{\sigma_z}{\sigma_0^2}},$$

where $\sigma_0 = \frac{\sigma_{rs}}{\rho}$; σ_{rs} – normalized RCS of the reflecting surface; ρ – density of point reflectors.

Both the complication and simplification of the model occurs by changing the density of the distribution of reflectors. It depends on what is more important for the researcher: to obtain the required accuracy or to achieve the specified speed of calculations. If you change the law of the distribution of reflectors in height, or change the parameters of this distribution law, you can get models with different reflective surfaces.

Background reflecting surfaces (RS) will be called statistically homogeneous areal formations of both natural and anthropogenic origin. The area of the RS should be significantly larger than the area of the radar resolution element S_r and local anthropogenic objects (AO) located on their background.

The reflection characteristics of RS as areal formations are described by the normalized RCS,

$$\sigma_0 = 4\pi D^2 \frac{I_{refl}}{I_{tx} S_r},$$

where *D* – the distance from the radar of the GBRC to the object; I_{tx} – the intensity of the emitted (incident) wave at a unit distance from the emitter; I_{refl} – the intensity of the reflected wave at a given viewing angle at a unit distance from the object; S_r – the area of the radar resolution element (RE) on the ground.

In turn, the intensity of the reflected signal can be represented as follows:

$$I_{refl} = I_{refl.bas.} + I_{refl.misc.},$$

where $I_{refl.bas.}$ – the main polarization component, in which reception and radiation are carried out on the same type of linear polarization: vertical or horizontal.

Then the propagation coefficient of the radio signal will be defined as

$$K_{tr} = \sum_{i=0}^{N-1} \frac{1}{d_{txm-zi} d_{zi-rxn}} e^{-jk_{rn}\left(d_{txm-zi} + d_{zi-rxn}\right) - \sigma_z(\varphi_1,\varphi_2)},$$

where *N* – the number of diffusers on a given surface area; d_{txm-zi} – the distance between the transmitter and the *i*-th reflector of the underlying surface; d_{zi-rxn} – the distance between the *i*-th reflector of the underlying surface and the receiver; $\sigma_z(\varphi_1,\varphi_2)$ – the value of the RCS of the *i*-th reflector when it is irradiated at an angle of φ_1 and the signal is received at an angle of φ_2:

$\sigma_z(\varphi_1,\varphi_2)=\sqrt{|\sigma_z(\varphi_1)||\sigma_z(\varphi_2)|}$, where $\sigma_z(\varphi)$ – the value of monostatic RCS depending on the irradiation angle.

4) Re-reflection of the radio signal first from the reflecting surface, and then from the target

$$K_{tr}=\frac{1}{d_{txm-zi}d_{z-c}d_{c-rxn}}e^{-jk_{rn}(d_{txm-zi}+d_{zi-c}+d_{ci-rxn})\Gamma(\varphi)},$$

where $\Gamma(\varphi)$ – reflection coefficient from the RS.

5) Re-reflection of the radio signal first from the target and then from the RS:

$$K_{tr}=\frac{1}{d_{txm-ci}d_{c-z}d_{z-rxn}}e^{-jk_{rn}(d_{txm-ci}+d_{c-z}+d_{z-rxn})\Gamma(\varphi)}.$$

Obviously, other types of trails not discussed above will not have a significant effect on the reflected signal, therefore, within the framework of the model under consideration, we can neglect them.

The total number of propagation paths for each *n*-th receiving and *m*-th transmitting module is defined as

$$K=2+3N.$$

Thus, taking into account the combinations of all receiving modules, propagation paths, transmitting modules and targets, a three-dimensional matrix of propagation coefficients $K_{trM\times N}$ is obtained, where N – total number of receiving modules, M – total number of transmission modules, K – total number of paths.

Taking into account all of the above, the final expression for the radio signal samples at the input of the *n*-th receiving module is as follows:

$$S_n(t_j)=\sum_{i=0}^{K-1}K_{tr}(t_j)\cdot X_n(t_j-\tau_k)\cdot(\tau_k-\tau_{k-i}),$$

where t_j – the time point at which the receiver input signal is calculated, τ_k – simulation time.

Assessment of the possibility of determining the density of obstacles by the radar channel of the on-board TVS of the GBRC

The above-described simulation model of the radar channel of the on-board TVS of the GBRC was developed in the Matlab mathematical programming environment and includes: an obstacle detection channel (a spatially distributed object) and a channel for measuring (evaluating) the received signal power.

The initial data for the model of the radar channel of the TVS of the GBRC for assessing the density of obstacles were:

– ypical obstacles and their dielectric characteristics [25];

– he size of the obstacle;

– distance to the obstacle;

– radar channel parameters of the on-board TVS of the GBRC.

The parameters of the radar channel of the on-board TVS of the GBRC during the assessment were:

– transmitting device power – P_{tx} = 1 W;

– operating frequency of the probe signal f_0 = 77 GHz;

– polarization of the probing signal – vertical;

– the probing signal is pulsed, modulated by a 63rd element Gold sequence;

– he width of the signal spectrum Π_s = 1 GHz;

– pulse duration T_i = 6.3 ns;

– pulse sending frequency F_s = 10 kHz;

– width of the antenna system's radiation pattern in the azimuthal plane $\Delta\beta$ = 0.5º;

– width of the antenna system's radiation pattern in the angular plane $\Delta\varepsilon$ = 0.5º;

– the type of space survey – consistent in azimuth and angle of location;

– antenna pattern scanning sector is ±30º by azimuth and 0-30º by location angle;

– height of the antenna system phase center – 1.5 m;

– noise factor of the receiving device – 3.

Studies to assess the possibility of determining the density of obstacles are carried out in the following sequence:

1) The operator downloads a simulation model of the radar channel of the TVS of the GBRC in the Matlab simulation environment;

2) the operator enters the initial data for the experiment (simulation), which includes:

- the type of obstacle, its size and dielectric characteristics;
- the required distance to the obstacle R_{ref}, at which it should be detected with a given probability and the density of obstacles estimated;
- the required probability of detecting an obstacle P_{det} and the probability of a false alarm P_{fa};
- power of the transmitting device P_{tx};
- the operating frequency of the probe signal f_0;
- polarization of the probe signal;
- probe signal type and modulation parameters;
- the width of the signal spectrum Π_s;
- duration of the signal T_s;
- the width of the radiation pattern of the transmitting and receiving antenna in the azimuthal ($\Delta\beta$) and angular planes ($\Delta\varepsilon$);
- height of the antenna phase center;
- signal polarization;
- the upper limit of the range measurement error σ_R;

3) the operator starts the process of simulating the functioning of the radar channel of the TVS of the GBRC in order to determine the density of obstacles;

4) по окончании моделирования оператор фиксирует выходные параметры модели радиолокационного канала of the TVS of the GBRC:

- radar portrait of an obstacle (spatially distributed object), as a function of the dependence of the received signal power normalized to the receiver noise level by resolution elements;

- the normalized RCS of the obstacle (spatially distributed object) σ_0 in each element of the resolution;
- the width of the spectrum of fluctuations of the received signal ΔF_{fl} and the correlation interval of the signal τ_{cor} in each element of the resolution;
- polarization characteristics of the received signal.

The normalized RCS of an obstacle in each element of the resolution σ_0 is calculated using a reference object with a known RCS and located at a known range using the formula:

$$\sigma_0 = \frac{P_{rx}\hat{R}^2_{meas}\sigma_{ref}\cos\theta}{P_{ref}R^4_{ref}\Delta R\Delta\beta\Delta\varepsilon},$$

where P_{rx} – the power of the signal received from the obstacle; $\hat{R}_{meas}$ – the measured distance to the obstacle; σ_{ref} – RCS of the reference object; R_{ref} – distance to the reference object; P_{ref} – signal power from the reference object; ΔR – range resolution; θ – obstacle exposure angle; $\Delta\beta$ – azimuth resolution; $\Delta\varepsilon$ – location angle resolution.

For each resolution element, the signal correlation interval is additionally calculated based on the results of receiving a sequence of echo signals during modeling τ_{cor}. The correlation interval τ_{cor} is an additional information parameter when assessing the type of obstacles by the radar channel of the TVS of the GBRC.

The simulation was performed at several frequencies using vertical and horizontal polarization of the signal.

The determination of the density (type) of an obstacle is carried out by comparing the simulation results obtained for determining the normalized RCS of obstacles with the data given in the reference literature on the normalized RCS of materials of different densities at appropriate frequencies and signal polarization [25].

For extended obstacles (spatially distributed objects), a radar portrait of the obstacle is formed, representing a $N_\beta \times N_\varepsilon$ matrix (where N_β, N_ε – the number of azimuth and location angle resolution elements, respectively), whose elements are the values of the received signal power normalized to the noise level of the receiving device.

The calculated values of the normalized RCS of the obstacle obtained as a result of experimental studies, the correlation time of the signal at the frequency f_0 (at a wind speed of 1 m/s) and the specified signal polarization are summarized in Table 1.

The results shown in Table 1 of the assessment of the possibility of determining the density of obstacles by the radar channel of the on-board TVS of the GBRC using a simulation model of the radar channel showed that the density of obstacles can be estimated by the normalized RCS of various obstacles. The normalized RCS of obstacles is determined with the least errors at short ranges (about 10-15 m). This is due to the fact that with a narrow antenna pattern at a short range, the signal is reflected from a small area of homogeneous material. As the range increases for non-uniform obstacles (such as a tree, shrub, tall grass), the density determination error increases.

Table 1

The results of the assessment of the possibilities of determining the density of obstacles by the radar channel of the on-board TVS of the GBRC

Type of obstacle/ Distance		Normalized RCS σ_0		Signal correlation time, s
		Reference [25]	Average calculated	
Dry tree	10 m	0.19	0.196	>10
	50 m	0.19	0.2	>10
Tree (separate)	10 m	0.33	0.24	0.7
	50 m	0.33	0.21	0.7
Shrub	10 m	0.17	0.18	0.051
	30 m	0.17	0.14	0.17
Grass	10 m	0.10	0.13	0.035
	30 m	0.17	0.12	0.12
Wall (concrete)	10 m	0.31	0.29	>10
	50 m	0.31	0.28	>10

This is determined by the fact that at long range, the geometric dimensions and the cross-sectional area of the beam increase, and the size of the resolution element increases accordingly. Within the beam, the reflecting surface becomes more heterogeneous due to the illumination of elements with different normalized RCS (for example, the trunk of a tree and the leaves of a crown).

As the simulation results have shown, certain types of obstacles (trees, shrubs, tall grass) can be additionally detected by the correlation time of the received signal, which is significantly lower than for homogeneous solid obstacles.

During the simulation, radar portraits of heterogeneous obstacles, such as a single tree, shrub, and tall grass, were obtained at ranges of 10-50 m. The radar portrait of an obstacle represents the dependence of the received signal power on the angular coordinates of the antenna pattern during a sequential survey of space. The more powerful signal in the drawing corresponds to the lighter color of the palette. The radar portraits of radar-contrasting objects (obstacles) obtained during the simulation are shown in Figures 1-5.

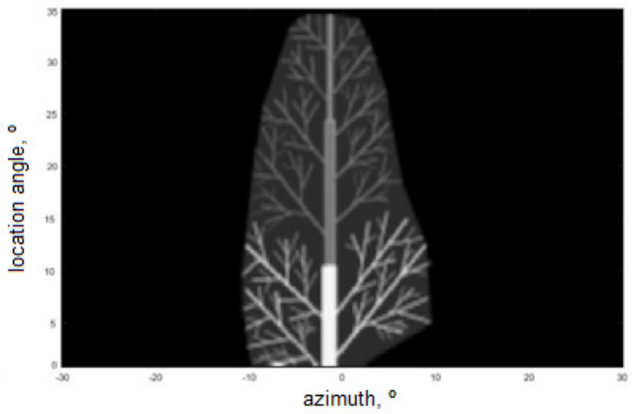

Figure 1. Radar portrait of a single tree (model) at a distance of 10 m

Figure 2. Radar portrait of a single tree (model) at a distance of 30 m

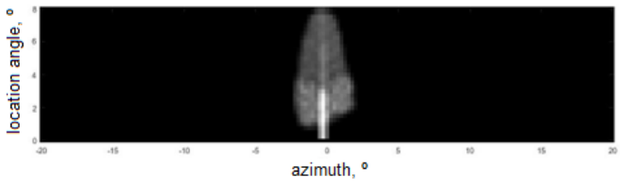

Figure 3. Radar portrait of a single tree (model) at a distance of 50 m

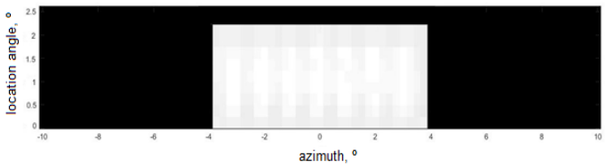

Figure 4. Radar portrait of an area with a shrub 3.9 m wide and 1.0 m high (model) at a distance of 10 m

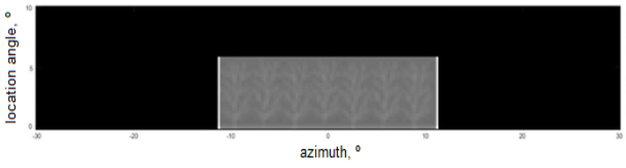

Figure 5. Radar portrait of an area with a shrub 3.9 m wide and 1.0 m high (model) at a distance of 30 m

Thus, the estimation of the obstacle density can be used as additional information in the TVS of the GBRC object recognition algorithm based on the well-proven Shortliffe scheme [26, 27]:

$$P_{\Sigma} = 1 - \prod_{i=1}^{N} \left(1 - P\left(A_i\right)\right),$$

where: N – number of measuring channels, A_i – information from the i-th channel, $P\left(A_i\right)$ – the probability of correct object recognition based on A_i. The algorithm diagram is shown in Figure 6.

In this scheme, information about the normalized RCS σ_0 and the signal correlation time τ_{cor} is used as additional features in the classification (recognition) of objects by radar measurements. The principle of using this information depends on the type of classifier (artificial neural network, decision tree, etc.). Further research by the authors will be devoted to the specific implementation of this algorithm.

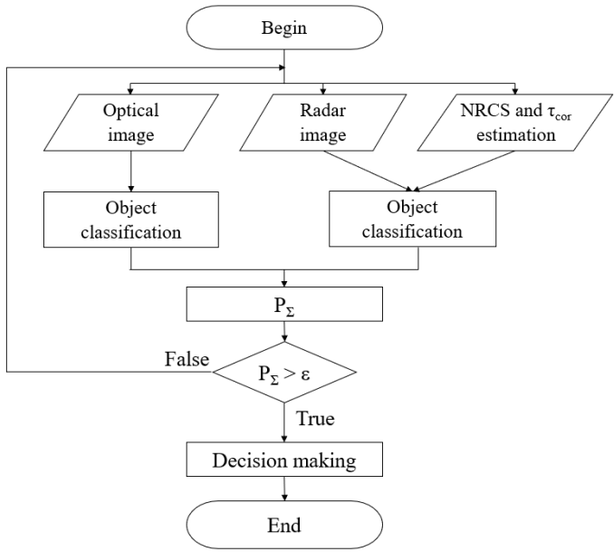

Figure 6. The scheme of the object recognition algorithm based on the Shortliffe scheme

Conclusion

The results of evaluating the possibility of determining the density of obstacles using the radar channel of the onboard TVS of the GBRC using a simulation model of the radar channel showed that the density of obstacles can be estimated based on the normalized RCS of various obstacles. The normalized RCS of obstacles is determined with the least errors at short distances (about 10-15 m).

Certain types of obstacles (trees, shrubs, and tall grass) can be further selected based on the correlation time of the received signal, which is significantly lower than that of homogeneous solid obstacles (wooden or concrete walls, and cars). During the simulation, radar portraits of heterogeneous obstacles, such as individual trees, shrubs, tall grass, and cars, were obtained at ranges of 10-50 m.

The results of evaluating radar portraits of radar-contrasting objects (obstacles) show that, with a high angular resolution of the radar channel, they can be classified using appropriate image recognition methods.

References

[1] I.S. Konstantinov and V.A. Gaivoronsky, “Formation of Area Data by Multi-Camera Video Systems”, *Economics. Computer Science*, 2022, No. 49(4), pp. 863–870, DOI: 10.52575/2687-0932-2022-49-4-863-870 (in Russian).

[2] D.N. Bezumnov, D.S. Chirov and M.V. Bazylev, “Object classification algorithm based on complex data processing of the technical vision system of a ground-based robotic complex”, *Telecommunications*, 2025, No. 2, pp. 40-45, DOI: 10.34832/ELSV.2025.64.2.006 (in Russian).

[3] P. Singh, S. Menkudale, S. Soni, V. Tank and A. Raj, "Comprehensive Survey on Radar Systems and Its Target Classification Techniques", *Journal of Electronics and Electrical Engineering*, 2025, No. 1, pp. 234-269, DOI: 10.37256/jeee.4120255934.

[4] P.V. Stepanov and D.S. Chirov, “Methods for identifying radio emission sources in an expert system for analyzing radio monitoring data”, *Issues of business control and financial audit, national security, system analysis, and management, Materials of the VII All-Russian Scientific and Practical Conference*, Moscow, Expert and Analytical Center, 2022, pp. 557-562 (in Russian).

[5] A.V. Nikonenko, D.S. Chirov and A.A. Kuchumov, “Appearance of a multi-beam radar system for detecting small air targets”, *Proceedings of the Research Institute of Radio Engineering*, 2023, No. 1, pp. 39-43, DOI 10.34832/NIIR.2023.12.1.005 (in Russian).

[6] D.N. Bezumnov, D.S. Chirov and O.V. Korenkov, “Method of information integration in technical vision systems of ground-based robotic systems”, *Issues of business control and financial audit, national security, system analysis, and management, Collection of Materials of the 10th All-Russian Scientific and Practical Conference*, Moscow, Expert and Analytical Center, 2024, pp. 460-467 (in Russian).

[7] A.M. Ageev, V.G. Bondarev and V.V. Protsenko, “Justification of the choice of radiation sources for a computer vision system in the problem of automatic landing of unmanned aerial vehicles”, *Computer Optics*, 2022, No. 46(2), pp. 239-245, DOI: 10.18287/2412-6179-CO-875 (in Russian).

[8] D.S. Chirov, O.G. Chertova and T.N. Potapchuk, “Methodology for justifying requirements for the technical vision system of a robotic complex”, *Proceedings of SPIIRAS*, 2017, No. 2 (51), pp. 152-176, DOI: 10.15622/sp.51.7. (in Russian).

[9] S.P. Khripunov and D.S. Chirov, “A methodological approach to justifying the feasibility of using intelligent information technologies in the synthesis of management models for complex organizational and technical systems”, *Information, Measurement and Control Systems*, 2016, vol. 14, No. 1, pp. 39-47. (in Russian).

[10] Y. Wang, X. Li, X. Yang, W. Qi, D. Zhang and J. Wang, “Estimation of Picea Schrenkiana Canopy Density at Sub-Compartment Scale by Integration of Optical and Radar Satellite Images”, *Forests*, 2024, No. 15, p. 1145, DOI: 10.3390/f15071145.

[11] D. Bibicu, A. Culea, S. Moldovanu and L. Moraru, “2D multiple waves scattering for active detection of a dummy human body in a low frequency range and for various boundary conditions”, *Journal of Physics: Conference Series*, 2024, No. 2701, p. 012012, DOI: 10.1088/1742-6596/2701/1/012012.

[12] D. Bibicu, S. Moldovanu and L. Moraru, “Numerical evaluation of low frequency sound propagation in two layered media”, *Journal of Physics: Conference Series*, 2019, No. 1391, p. 012032, DOI: 10.1088/1742-6596/1391/1/012032.

[13] S. Skaria, N. Hendy and A. Al-Hourani, “Machine Learning Methods for Material Identification Using mmWave Radar Sensor”, *IEEE Sensors Journal*, 2022, pp. 1-1, DOI: 10.1109/JSEN.2022.3227207.

[14] C. He, J. Song and H. Xu, "Optical and SAR Data Fusion Based on Transformer for Rice Identification: A Comparative Analysis from Early to Late Integration", *Agriculture*, 2025, No. 15, p. 706, DOI: 10.3390/agriculture15070706.

[15] B. Jamali, D. Ramalingam and A. Babakhani, “Intelligent Material Classification and Identification Using a Broadband Millimeter-Wave Frequency Comb Receiver”, *IEEE Sensors Letters*, 2020, pp. 1-1, DOI: 10.1109/LSENS.2020.3002715.

[16] C. Bhattacharya, J. Singh, D. Sahu, V. Mor, A. Kumar and S. Ravindra, "Real-Time product quality assurance management Using Vision sensor and Convolutional Neural Networks", *International Conference on Data Processing and Networking (ICDPN-2024)*, 2025, DOI: 10.1007/978-981-96-3102-5_21.

[17] J. Weiß and A. Santra, “One-Shot Learning for Robust Material Classification Using Millimeter-Wave Radar System”, *IEEE Sensors Letters*, 2018, pp. 1-1, DOI: 10.1109/LSENS.2018.2878041.

[18] A. Soumya, K.M. Chalavadi and L.R. Cenkeramaddi, “Recent Advances in mmWave-Radar-Based Sensing, Its Applications, and Machine Learning Techniques: A Review”, *Sensors*, 2023, p. 23, DOI: 10.3390/s23218901.

[19] J. Chan, P. Evans, X. Wang, S. Godber, I. Peatfield, K. Rogers, J. Rogers and A. Dicken, “Scatter enhanced 3D X-ray imaging for materials identification”, *Proceedings – International Carnahan Conference on Security Technology*, 2010, pp. 142-147, DOI: 10.1109/CCST.2010.5678684.

[20] G. Dobmann, I. Altpeter, C. Sklarczyk and R. Pinchuk, “Non-destructive testing with micro- and Mm-waves – where we are – where we go”, *Fraunhofer IZFP*, 2013, No. 56, DOI: 10.1007/BF03321153.

[21] M. Shehab, M. Alkaltakchi, A. Dukhan and W.L. Woo, "Enhancing Ground Penetrating Radar (GPR) Data Analysis Utilizing Machine Learning", *Journal of Engineering and Sustainable Development*, 2025, No. 29, pp. 321-330, DOI: 10.31272/jeasd.2509.

[22] L. Lasantha, B. Ray, H. Masoumi and N. Karmakar, "Cross-Polarised Chipless RFID Sensor: A Novel Approach for Measuring Dielectric Constants in Solid Minerals and Rocks", *IEEE Sensors Journal*, 2025, pp. 1-1, DOI: 10.1109/JSEN.2025.3565761.

[23] K. Shi, Z. Shi, A. Chen, Z. Xiong, J. Chen and J. Luo, "Radar and Camera Fusion for Object Detection and Tracking: A Comprehensive Survey", *IEEE Communications Surveys & Tutorials*, 2024.

[24] Yu.S. Nefedova and A.A. Karankevich, “Development of a propagation channel model for a multi-position radar system”, *Radar, Navigation, and Communication: Proceedings of the 16th International Scientific and Technical Conference*, Voronezh, 2010, vol. 3, pp. 1812-1819 (in Russian).

[25] V.A. Pavelyev and D.V. Khaminov, “Scattering of millimeter-wave electromagnetic radiation by natural and anthropogenic objects”, edited by Dr. V.L. Solunin, Moscow, Bauman Moscow State Technical University Publishing House, 2009, 277 p. (in Russian).

[26] D.N. Bezumnov and D.S. Chirov, “On Improving the Efficiency of the Technical Vision System of the Robotics Complex”, *2025 Systems of Signals Generating and Processing in the Field of on Board Communications*, Moscow, Russian Federation, 2025, pp. 1-4, DOI: 10.1109/IEEECONF64229.2025.10948107.

[27] D.N. Bezumnov and D.S. Chirov, “Object recognition method based on complex data processing of the technical vision system of a ground-based unmanned vehicle”, *Digital signal processing*, 2025, No. 2, pp. 36-39 (in Russian).

[28] S.S. Adjemov, E.M. Lobov, N.A. Kandaurov, E.O. Lobova, V.I. Lipatkin, “Algorithms of estimating and compensating the dispersion distortions of wideband signals in the HF channel,” *H&ES Reserch*. 2021. Vol. 13. No. No.5, pp. 57-74. doi: 10.36724/2409-5419-2021-13-5-57-74 (In Rus)

[29] D.S. Chirov, E.O. Lobova, “Wideband HF signals dispersion distortion compensator based on digital filter bank. Theory and approbation,” *T-Comm*. 2020. Vol. 14. No. 4, pp. 57-65.

[30] O.G. Chertova, D.S. Chirov, “Building a core communication network which is based on small size unmanned aircraft vehicle without ground infrastructure,” *H&ES Research*. 2019. Vol. 11. No. 3, pp. 60-71. doi: 10.24411/2409-5419-2018-10269

[31] D.S. Chirov., E.M. Lobov, “Choice of signal-code constructure for the command-telemetry radio communication line with medium and long range unmanned aerial vehicles,” *T-Comm*, 2017, vol. 11, no.10, pp. 21-28.

ОЦЕНКА ПЛОТНОСТИ ПРЕПЯТСТВИЯ ПО ИЗМЕРЕНИЯМ РАДИОЛОКАЦИОННОГО КАНАЛА СИСТЕМЫ ТЕХНИЧЕСКОГО ЗРЕНИЯ НАЗЕМНОГО РОБОТОТЕХНИЧЕСКОГО КОМПЛЕКСА

Безумнов Данил Николаевич, *Московский технический университет связи и информатики, Москва, Россия,* ***d.n.bezumnov@mtuci.ru***

Чиров Денис Сергеевич, *Московский технический университет связи и информатики, Москва, Россия,* ***d.s.chirov@mtuci.ru***

Аннотация

Одним из основных трендов развития робототехники является повышение автономности и интеллектуализации робототехнических комплексов. Основным источникам данных для принятия решения и осуществления тех или иных действий РТК является система технического зрения. Поэтому совершенствование СТЗ и алгоритмов обработки данных от нее является важной задачей. В статье представлены результаты исследований по оценки плотности препятствия по измерениям радиолокационного канала системы технического зрения наземного робототехнического комплекса. Данная задача актуальна при автономном построении маршрута наземного РТК, т.е. когда НРТК строит маршрут самостоятельно из точки А в точку В и корректирует его в случае обнаружения препятствий. Очевидно, что в случае применения НРТК в сельской местности, оптический канал воспримет высокую траву как препятствие и начнет перестраивать маршрут, что может привести к удлинению пути или, в конечном счет, не выполнения задачи НРТК. Анализ существующих исследований показал, что оценить плотность препятствия возможно с использованием измерений РЛС мм-диапазона. Результаты оценки возможности определения плотности препятствий радиолокационным каналом бортовой СТЗ НРТК с использованием имитационной модели радиолокационного канала показали, что плотность препятствий может быть оценена по удельной ЭПР различных препятствий. Удельная ЭПР препятствий с наименьшими ошибками определяется на небольших дальностях (порядка 10-15 м). Отдельные типы препятствий (деревья, кустарники, высокая трава) могут быть дополнительно отселектированы по времени корреляции принятого сигнала, которое у них значительно ниже, чем у однородных твердых препятствий (стены из дерева или бетона, автомобиль). Принцип использования удельной ЭПР и времени корреляции сигнала зависит от типа классификатора (искусственная нейронная сеть, дерево решений и т.п.). Конкретной реализации данного алгоритма будут посвящены дальнейшие исследования авторов.

Ключевые слова: *робототехнический комплекс, система технического зрения, радиолокационные измерения, обработка информации, распознавание объектов.*

Литература

1. *Константинов И.С., Гайворонский В.А.* Формирование данных о пространстве многокамерными видеосистемами // Экономика. Информатика. 2022. № 49(4). С. 863-870. DOI 10.52575/2687-0932-2022-49-4-863-870.

2. *Безумнов Д.Н., Чиров Д.С., Базылев М.В.* Алгоритм классификации объектов на основе комплексной обработки данных системы технического зрения наземного робототехнического комплекса // Электросвязь. 2025. № 2. С. 40-45. DOI: 10.34832/ELSV.2025.64.2.006.

3. *Singh P., Menkudale S., Soni S., Tank V., Raj A.* Comprehensive Survey on Radar Systems and Its Target Classification Techniques // Journal of Electronics and Electrical Engineering, 2025, No. 1, pp. 234-269, DOI: 10.37256/jeee.4120255934.

4. *Степанов П.В., Чиров Д.С.* Методы идентификации источников радиоизлучения в экспертной системе анализа данных радиомониторинга // Вопросы контроля хозяйственной деятельности и финансового аудита, национальной безопасности, системного анализа и управления : материалы VII Всероссийской научно-практической конференции, Москва, 29 декабря 2021 г. М.: ФГБНУ "Экспертно-аналитический центр", 2022. С. 557-562.

5. *Никоненко А.В., Чиров Д.С., Кучумов А.А.* Облик многолучевой РЛС обнаружения малоразмерных воздушных целей // Труды Научно-исследовательского института радио. 2023. № 1. С. 39-43. DOI 10.34832/NIIR.2023.12.1.005.

6. *Безумнов Д.Н., Чиров Д.С., Кореньков О.В.* Метод комплексирования информации в системах технического зрения наземных робототехнических комплексов // Вопросы контроля хозяйственной деятельности и финансового аудита, национальной безопасности, системного анализа и управления : Сборник материалов X Всероссийской научно-практической конференции, Москва, 07 ноября 2024 года. М.: ФГБНУ "Экспертно-аналитический центр", 2024. С. 460-467.

7. *Агеев А.М., Бондарев В.Г., Проценко В.В.* Обоснование выбора источников излучения для системы технического зрения в задаче автоматической посадки беспилотных летательных аппаратов // Компьютерная оптика. 2022. Т. 46. № 2. С. 239-245. DOI: 10.18287/2412-6179-CO-875.

8. *Чиров Д.С., Чертова О.Г., Потапчук Т.Н.* Методика обоснования требований к системе технического зрения робототехнического комплекса // Труды СПИИРАН. 2017. № 2 (51). С. 152-176. DOI: 10.15622/sp.51.7.

9. *Хрипунов С.П., Чиров Д.С.* Методический подход по обоснованию целесообразности применения интеллектуальных информационных технологий при синтезе моделей управления сложными организационно-техническими системами // Информационно-измерительные и управляющие системы. 2016. Т. 14. № 1. С. 39-47.

10. Wang Y., Li X., Yang X., Qi W., Zhang D., Wang J. Estimation of Picea Schrenkiana Canopy Density at Sub-Compartment Scale by Integration of Optical and Radar Satellite Images // Forests, 2024, No. 15, p. 1145, DOI: 10.3390/f15071145.

11. *Bibicu D., Culea A., Moldovanu S., Moraru L.* 2D multiple waves scattering for active detection of a dummy human body in a low frequency range and for various boundary conditions // Journal of Physics: Conference Series, 2024, No. 2701, p. 012012, DOI: 10.1088/1742-6596/2701/1/012012.

12. *Bibicu D., Moldovanu S., Moraru L.* Numerical evaluation of low frequency sound propagation in two layered media // Journal of Physics: Conference Series, 2019, No. 1391, p. 012032, DOI: 10.1088/1742-6596/1391/1/012032.
13. *Skaria S., Hendy N., Al-Hourani A.* Machine Learning Methods for Material Identification Using mmWave Radar Sensor // IEEE Sensors Journal, 2022, pp. 1-1, DOI: 10.1109/JSEN.2022.3227207.
14. *He C., Song J., Xu H.* Optical and SAR Data Fusion Based on Transformer for Rice Identification: A Comparative Analysis from Early to Late Integration // Agriculture, 2025, No. 15, p. 706, DOI: 10.3390/agriculture15070706.
15. *Jamali B., Ramalingam D., Babakhani A.* Intelligent Material Classification and Identification Using a Broadband Millimeter-Wave Frequency Comb Receiver // IEEE Sensors Letters, 2020, pp. 1-1, DOI: 10.1109/LSENS.2020.3002715.
16. *Bhattacharya C., Singh J., Sahu D., Mor V., Kumar A., Ravindra S.* Real-Time product quality assurance management Using Vision sensor and Convolutional Neural Networks // International Conference on Data Processing and Networking (ICDPN-2024), 2025, DOI: 10.1007/978-981-96-3102-5_21.
17. *Weiss J., Santra A.* One-Shot Learning for Robust Material Classification Using Millimeter-Wave Radar System // IEEE Sensors Letters, 2018, pp. 1-1, DOI: 10.1109/LSENS.2018.2878041.
18. *Soumya A., Chalavadi K.M., Cenkeramaddi L.R.* Recent Advances in mmWave-Radar-Based Sensing, Its Applications, and Machine Learning Techniques: A Review // Sensors, 2023, p. 23, DOI: 10.3390/s23218901.
19. *Chan J., Evans P., Wang X., Godber S., Peatfield I., Rogers K., Rogers J., Dicken A.* Scatter enhanced 3D X-ray imaging for materials identification // Proceedings - International Carnahan Conference on Security Technology, 2010, pp. 142-147, DOI: 10.1109/CCST.2010.5678684.
20. *Dobmann G., Altpeter I., Sklarczyk C., Pinchuk R.* Non-destructive testing with micro- and Mm-waves - where we are - where we go // Fraunhofer IZFP, 2013, No. 56, DOI: 10.1007/BF03321153.
21. *Shehab M., Alkaltakchi M., Dukhan A., Woo W.L.* Enhancing Ground Penetrating Radar (GPR) Data Analysis Utilizing Machine Learning // Journal of Engineering and Sustainable Development, 2025, No. 29, pp. 321-330, DOI: 10.31272/jeasd.2509.
22. *Lasantha L., Ray B., Masoumi H., Karmakar N.* Cross-Polarised Chipless RFID Sensor: A Novel Approach for Measuring Dielectric Constants in Solid Minerals and Rocks // IEEE Sensors Journal, 2025, pp. 1-1, DOI: 10.1109/JSEN.2025.3565761.
23. *Shi K., Shi Z., Chen A., Xiong Z., Chen J., Luo J.* Radar and Camera Fusion for Object Detection and Tracking: A Comprehensive Survey // IEEE Communications Surveys & Tutorials, 2024.
24. *Нефедова Ю.С., Каранкевич А.А.* Разработка модели канала распространения многопозиционной радиолокационной системы // Радиолокация, навигация, связь: Труды XVI международной научно-технической конференции. Воронеж, 2010. Т. 3. С. 1812-1819.
25. *Павельев В.А., Хаминов Д.В.* Рассеяние электромагнитных волн миллиметрового диапазона природными и антропогенными объектами / под ред. д-ра техн. наук В.Л. Солунина. М.: Изд-во МГТУ им. Н. Э. Баумана, 2009. 277 с.
26. *Bezumnov D.N., Chirov D.S.* On Improving the Efficiency of the Technical Vision System of the Robotics Complex // 2025 Systems of Signals Generating and Processing in the Field of on Board Communications, Moscow, Russian Federation, 2025, pp. 1-4, DOI: 10.1109/IEEECONF64229.2025.10948107.
27. *Безумнов Д.Н., Чиров Д.С.* Метод распознавания объектов на основе комплексной обработки данных системы технического зрения наземного беспилотного транспортного средства // Цифровая обработка сигналов. 2025. № 2. С. 36-39.
28. *Аджемов С.С., Лобов Е.М., Кандауров Н.А., Лобова Е.О., Липаткин В.И.* Алгоритмы оценки и компенсации дисперсионных искажений широкополосных сигналов ионосферных радиолиний связи // Наукоемкие технологии в космических исследованиях Земли. 2021. Т. 13. № 5. С. 57-74.
29. *Chirov D.S., Lobova E.O.* Wideband HF signals dispersion distortion compensator based on digital filter banks. Theory and approbation // T-Comm. 2020. Т. 14. № 4. С. 57-65.
30. *Чертова О.Г., Чиров Д.С.* Построение опорной сети связи на базе малоразмерных беспилотных летательных аппаратов с отсутствием наземной инфраструктуры // Наукоемкие технологии в космических исследованиях Земли. 2019. Т. 11. № 3. С. 60-71.
31. *Чиров Д.С., Лобов Е.М.* Выбор сигнально-кодовой конструкции для командно-телеметрической линии радиосвязи с беспилотными летательными аппаратами средней и большой дальности // T-Comm: Телекоммуникации и транспорт. 2017. Т. 11. № 10. С. 21-28.

Информация об авторах:

Безумнов Данил Николаевич, *старший преподаватель, Московский технический университет связи и информатики, Москва, Россия*

Чиров Денис Сергеевич, *заведующий кафедрой, доктор технических наук, профессор, Московский технический университет связи и информатики, Москва, Россия*